Editors' Suggestion

Effect of inertial migration of particles on flow transitions of a suspension Taylor-Couette flow

Lina Baroudi*
Department of Mechanical Engineering, Manhattan College, Bronx, New York 10471, USA

Madhu V. Majji
Department of Chemical Engineering, Massachusetts Institute of Technology, Cambridge, Massachusetts 02139, USA

Jeffrey F. Morris
Levich Institute and Department of Chemical Engineering, CUNY City College of New York, New York, New York 10031, USA

(Received 9 August 2020; accepted 6 October 2020; published 11 November 2020)

The influence of inertial migration of neutrally buoyant particles on inertial flow transitions in Taylor-Couette (TC) flow of a suspensions is studied; this work considers primarily transitions associated with the circular Couette flow (CCF) and Taylor vortex flow (TVF) regimes. A concentric cylinder Taylor-Couette device with a stationary outer cylinder and rotating inner cylinder is considered. The device has an inner to outer radius ratio of $\eta = d_i/d_o = 0.877$, where d_i and d_o are the inner and outer diameters of the flow annulus. The ratio of the axial length to the radial gap of the annulus $\Gamma = L/\delta = 20.5$, where $\delta = (d_o - d_i)/2$. The ratio of radial gap δ and the particle diameter d_p is $\alpha = \delta/d_p = 30.4$ and the particle volume fraction considered in this work is $\phi = 0.10$. A flow structure (CCF or TVF) near the transition boundary with either uniform distribution across the annular region or fully migrated concentration profile is established. The Reynolds number (Re) is subjected to a rapid step change to study the effect of the concentration profile on the flow transition Re and resulting flow structure evolution; here the Reynolds number is $\mathrm{Re} = \delta d_i \omega_i \rho / 2\mu_s$, where ω_i is the rotation rate of the inner cylinder and ρ and μ_s are the density and effective viscosity of the suspension. Our results show that, relative to uniform concentration, the particle distribution following inertial migration destabilizes the CCF state near the CCF-nonaxisymmetric flow transition boundary. In contrast to this destabilizing effect in CCF, migration of particles in the TVF regime has a stabilizing effect on the TVF-wavy Taylor vortex and TVF-nonaxisymmetric flow transition boundaries. The transition away from the TVF exhibits clear hysteresis associated with migration, as once initiated TVF could be sustained below and above the transition boundaries observed for suspension TC flow with uniform concentration.

DOI: 10.1103/PhysRevFluids.5.114303

I. INTRODUCTION

The Taylor-Couette flow (TCF) between concentric rotating cylinders offers a fertile ground for examination of instability phenomena. It is well known that the flow in the annular region displays different flow structures ranging from unidirectional shear flow through a number of vortex flows

*lina.baroudi@manhattan.edu

to fully developed turbulent flow depending on inner and outer cylinder rotation rates. The various flow transitions and flow structures of a pure Newtonian fluid in TCF have been investigated in many experimental, theoretical, and numerical studies [1–9]. Considerable work has also been done to probe the flow transitions of non-Newtonian fluids in this flow [10–13]. More recently, inertial instabilities of suspension TCF have been shown to exhibit rich and complex dynamical behavior that are not readily explained by effective medium approaches [14,15].

For a suspension in the dilute limit ($\phi < 0.05$), linear stability analysis performed by Ali *et al.* [16] predicted that the particles destabilize the circular Couette flow. However, in this same study, experiments with neutrally buoyant particles for concentrations $\phi < 0.005$ showed a stabilizing effect of the particles, in contrast to the predictions. More recently, Majji *et al.* [14] carried out experimental study of the effect of particle loading and size on inertial flow transitions of a neutrally buoyant suspension in TCF (inner to outer cylinder radius ratio of $\eta = 0.877$) for the case in which only the inner cylinder rotates. With increasing Reynolds number Re (definition in the following section), a pure fluid undergoes transitions from the purely azimuthal circular Couette flow (CCF) to Taylor vortex flow (TVF) to azimuthally propagating wavy Taylor vortex (WTV) flow. For dilute suspensions with $\phi < 0.05$, flow transitions follow the same sequence as in the pure fluid (CCF $\leftrightarrow$ TVF $\leftrightarrow$ WTV).

For higher ϕ, however, the transitions differ qualitatively from those observed in pure fluids. For $0.05 < \phi < 0.15$, nonaxisymmetric flow (NAF) states, namely spiral vortex flow (SVF) and ribbons (RIB), were uncovered at Re between those associated with TVF and CCF. For $\phi = 0.20$ and $\phi = 0.30$, a nonaxisymmetric flow structure called wavy spiral vortex flow (WSV) was observed at higher rotation rate. All of the nonaxisymmetric flow (NAF) structures described [14] are absent in a pure Newtonian fluid with only the inner cylinder rotating. The values of Re corresponding to flow transitions in the suspension were observed to become smaller with increase in particle loading, implying an early onset of primary instabilities compared to the Newtonian fluid. Subsequently, Ramesh *et al.* [15] conducted experiments on suspension TCF, performing simultaneous flow visualization and velocity measurements using particle image velocimetry (PIV). These authors found clear evidence of hysteresis, reporting that the sequence of flow transitions with an increasing-Re ramp is qualitatively different from transitions observed for decreasing Re. They observed a sequence of flow transitions of WTV $\rightarrow$ TVF $\rightarrow$ SVF $\rightarrow$ CCF with quasisteady decreasing-Re ramp and found two new coexisting states, namely (i) WTV with TVF and (ii) TVF with SVF in a quasisteady increasing-Re ramp experimental protocol. In recent work, Ramesh *et al.* [17] conducted experiments in a Taylor-Couette cell with a larger ratio of the axial length to annular gap and reported a new pattern called interpenetrating spiral vortices (ISVs), a coexisting state of upward and downward propagating spirals. The ISV state was found for both increasing- and decreasing-Re ramps.

One factor that differs significantly from Newtonian fluids is that particles can migrate and lead to spatial variation of the fluid properties. Particles in dilute suspensions flowing at finite Reynolds number in spatially varying shear flows are known to undergo inertial migration. This was first reported by Segré and Silberberg [18,19] for pressure-driven (Poiseuille) flow in a pipe, with subsequent study of inertial migration in different flow geometries [20–23]. The phenomenon of inertial particle migration should be distinguished from rheologically driven migration that is important at higher solid fraction [24]. We choose to consider the TC flow to study migration of particles in different flow structures and its effect on flow instabilities. A primary motivation is that this is a flow for which inertial transitions are well known, and thus the role of migration can be examined through comparison of nonuniform suspension behavior against that of uniform suspensions and pure fluids. The nonuniform concentration profiles lead to two rheological effects: viscosity variation across the annular width and fluctuating motions that result in added inertial stresses (Reynolds stresses) [25]. Majji *et al.* [14] performed linear stability analysis of the circular Couette flow with an elevated viscosity at the center of the annulus, corresponding to an approximation of the concentration profile following migration. For $\phi_{\text{avg}} = 0.10$, their analysis predicted that the modified viscosity profile due to migration stabilizes the CCF state compared to the uniform viscosity case. This disagrees

with their experiments, which showed neutrally buoyant particles destabilize the flow (as do our experiments in the current work). They postulated that since a simple viscosity gradient stabilizes the flow, the destabilizing effect may arise from the noted particle Reynolds stresses. Here, rather than exploring the mechanism of destabilization, we consider the fact that migration induces a history dependence and thus a significant hysteresis as described previously [14,15] and developed here in discussion of Fig. 4.

This source of hysteresis is due to the particulate distribution resulting from migration. Inertial migration results from the forces generated by the shear gradient and particle-induced flow disturbances with the solid boundaries, and consequently the particle distribution differs markedly with the carrying flow considered. Halow *et al.* [26] observed that neutrally buoyant spheres in circular Couette flow migrate to an equilibrium position near the middle of the annular gap. In TVF of dilute suspensions, Wereley *et al.* [27] integrated point-particle trajectories, ignoring the inertial migration due to finite particle size, to show that neutrally buoyant particles follow the TVF streamlines whereas particles heavier than fluid migrate to a limit cycle orbit around the vortex center irrespective of whether they start near the vortex center or the cylinder walls. In more recent work, Majji *et al.* [28] showed that neutrally buoyant uniformly distributed particles in the circular Couette flow (CCF) migrate to an equilibrium radial location, which is 0.4δ from the inner cylinder (δ is the annular width); in TVF, randomly distributed neutrally buoyant particles in the annular region were observed to migrate to a circular equilibrium location in the radial-axial (r-z) plane in each vortex, with the circle size varying with Re. In WTV, the particles were apparently homogeneously distributed across the annular gap. At intermediate and high concentrations, the particle-particle hydrodynamic interactions along with inertial migration have been shown in pressure-driven flow to lead to nonuniform distribution of particles and modified velocity profiles [29].

While the effect of suspended particles on inertial flow transitions was recently investigated, the role of inertial migration of particles on inertial flow transitions and observed flow structures has not been established for Taylor-Couette flow. In the present work, we consider the hysteresis effects associated with particles by focusing on the effect of particle migration in the CCF and TVF regimes on inertial flow transitions away from these initial states.

II. EXPERIMENT

A. Apparatus and materials

The Taylor-Couette apparatus used in this study consists of two vertical coaxial cylinders, the inner made of solid aluminum and the outer transparent acrylic. The apparatus is schematically illustrated in Fig. 1. The inner and outer diameters of the resulting fluid annulus are $d_i = 100.3$ mm and $d_o = 114.3$ mm, respectively. The width of the annular gap is $\delta = (d_o - d_i)/2 = 7$ mm and its height is $L = 144$ mm. The radius ratio is $\eta = d_i/d_o = 0.877$, and the ratio of the height to the annular gap is $\Gamma = L/\delta = 20.5$. The outer cylinder was held fixed, and the inner cylinder rotation was driven by a stepper motor (Lin Engineering, Silverpak 23C: CO-5718M-02P), connected to the cylinder shaft using a flexible coupling. The angular velocity and angular acceleration of the inner cylinder were controlled using a MATLAB-based computer interface. Water at 20 °C was circulated through a rectangular acrylic cooling jacket around the outer cylinder during the experiment to maintain uniform and constant temperature of the working fluid. The working fluid is a neutrally buoyant suspension of spherical particles of poly (methyl methacrylate), or PMMA, with density 1.18 g cm^{-3}. The particles were sieved to obtain a size distribution of approximately $212 < d_p < 250$ μm (mean $d_p \approx 230$ μm). The ratio of the annular width to the mean particle diameter $\alpha = \delta/d_p = 30.4$. For each experiment, the suspending fluid was prepared by mixing water and glycerol in a 1 : 2 weight ratio to match the fluid density to that of the particles at 20 °C. A small quantity (0.04% by volume) of the surfactant Triton X-100 (Sigma Aldrich) was added to the suspension to reduce interfacial tension and thus reduce particle adhesion to the air-water interface. For the purpose of visualization of flow structures, 0.05% by volume of Pearl Swirl (Steve Spangler

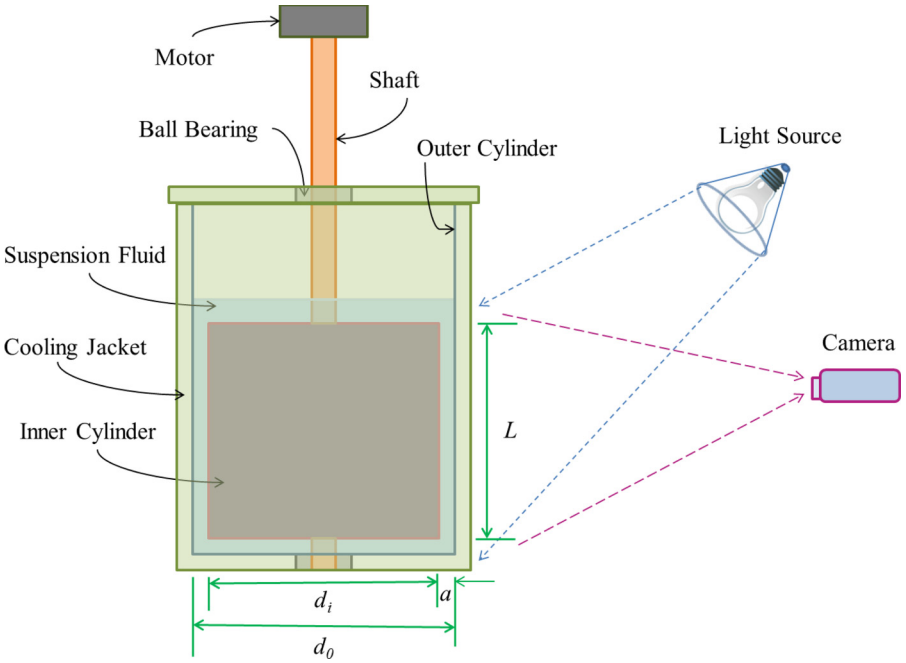

FIG. 1. Schematic of the experimental apparatus.

Science) made of 1% by volume of flakes in aqueous solution was added to the fluid mixture; these flakes are composed of a mixture of titanium dioxide and crystalline silica and are 12 μm in the largest dimension and much thinner in the perpendicular dimension. When illuminated from the top at an angle as indicated in Fig. 1, the flakes reflect light toward the camera at different intensities depending on their orientation. This variation in the reflected light intensity is recorded by two cameras for each experiment: (i) a high speed camera (Photron FASTCAM 1024 PCI) to record 60 frames s^{-1} for up to five s, and (ii) a low speed camera (Dino-Lite) to record at less than 1 frame s^{-1} for longer durations. Particles and suspending fluid were mixed to make suspensions of 10% concentration, and a volume of 500 mL was placed inside the annulus to submerge the inner cylinder by 18 mm.

The Reynolds number based on the inner cylinder rotation rate ω_i is given as $\mathrm{Re} = \delta d_i \omega_i \rho / 2\mu_s$, where ρ and μ_s are the density and effective viscosity of the suspension, respectively. Measured suspension viscosities followed very closely the Krieger correlation, $\mu_s = \mu_l(1 - \phi/\phi_m)^{-1.82}$ with $\phi_m = 0.55$, where μ_l is the viscosity of the fluid mixture without particles. The particle Reynolds number is given by $\mathrm{Re}_p = \mathrm{Re}(d_p/2\delta)^2 = O(0.01)$ for the conditions studied. Photographs of different flow structures observed for a $\phi = 0.10$ suspension of $d_p \approx 230$ μm are displayed in Fig. 2. The flow states shown are CCF at Re = 100.5, SVF at Re = 111.8, TVF at Re = 121.2, and WTV at Re = 140.0. Note that RIB state is not shown in Fig. 2.

B. Experimental procedures

1. Experimental protocol: Re step change experiments

The inertial migration in dilute suspensions has been previously studied in the apparatus used in the current study [28], and was found to depend on the underlying flow type (CCF or TVF) and flow duration. The migration drives the particles from a uniformly distributed state to accumulate at specific equilibrium locations. At the moderate particle concentrations studied in the current work, $\phi = 0.10$, the inertial migration results in regions of larger concentration where the resulting flow

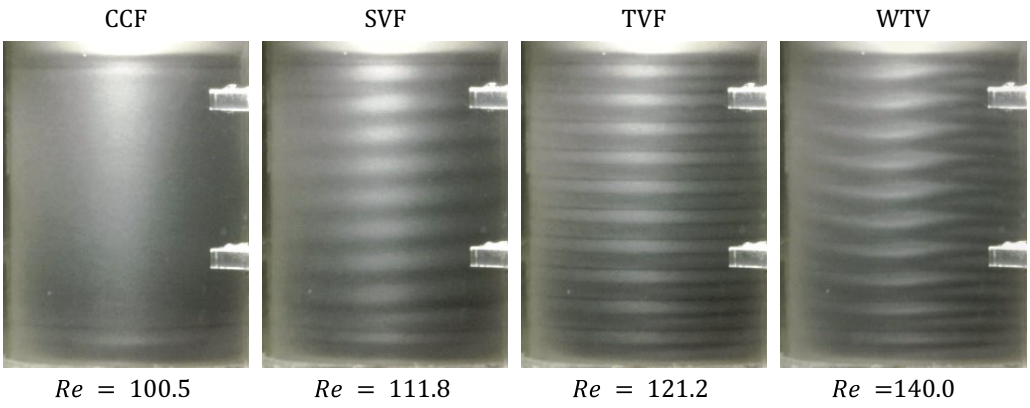

FIG. 2. Photographs of flow structures for a $\phi = 0.10$ suspension of $d_p \approx 230$ μm, from left to right: CCF, SVF, TVF, and WTV at Re = 100.5, 111.8, 121.2, and 140.0, respectively. The RIB state is not shown.

disturbances created by the particles in shear flow will tend to disperse the particles relative to the sharp localized distribution at more dilute ϕ studied in the noted earlier work [28]. The objective here is to study the effect of the nonuniform concentration profiles on hysteretic behavior. We do this by considering the influence of migration in the initial flow state on both the flow transition and final flow state when the rotation rate is changed at a rapid rate (in about two seconds) from Re_1 to Re_2, where Re_1 and Re_2 are in the vicinity of transition boundary.

Two concentration profiles in the initial state at Re_1 are studied: (I) negligible migration: nearly uniform concentration profile obtained by waiting only for 1 min at Re_1, and thus not allowing time for significant inertial migration to occur; (II) full migration: steady concentration profiles after allowing enough time (50 min) for inertial migration to take place, based on migration rates deduced from prior work [28] and our own experiments described below. From the several currently known flow transitions for suspension TC flow, we focused on the effect of the two concentration profiles in the following three scenarios. (i) Starting with an initial flow state at Re_1 in CCF regime near the transition boundary, the Reynolds number is increased quickly to Re_2. (ii) Starting from Re_1 in the TVF regime near the TVF-WTV transition boundary followed by a rapid step increase in Re. (iii) Starting from Re_1 in the TVF regime near transition boundary between TVF and nonaxisymmetric (NAF) flow states followed by rapid step decrease in Re. In each of these scenarios, we will show that the concentration profile of the initial state had a significant impact, not only on the transition Re but also on the final flow state.

To arrive at a consistent initial state with uniform concentration for all experiments presented, the following procedure was followed. The inner cylinder was first rotated at Re = 180 to establish WTV and held for 120 s to allow adequate particle mixing to achieve a uniformly distributed particle state. The inner cylinder was then stopped and held stationary for 120 s to ensure no residual flow before each experiment. The rotation rate of the inner cylinder was increased very rapidly from rest to Re_1 corresponding to the required flow state (CCF or TVF). For the experiments discussed in this work, the step change in Re is between 3% and 8% of Re_1.

2. Establishing the time required for complete inertial migration

Inertial migration time scales required for a uniformly distributed concentrated profile to reach an equilibrium concentration profile in CCF and TVF regimes were determined by conducting experiments with dilute suspensions of PMMA particles ($\phi = 0.01$ and $d_p \approx 230$ μm). Figure 3 shows snapshots from the final steady particle distributions in CCF at Re = 70 and in TVF at Re = 128. Note that the illuminating fluid (Pearl Swirl) was not used in these experiments. Images

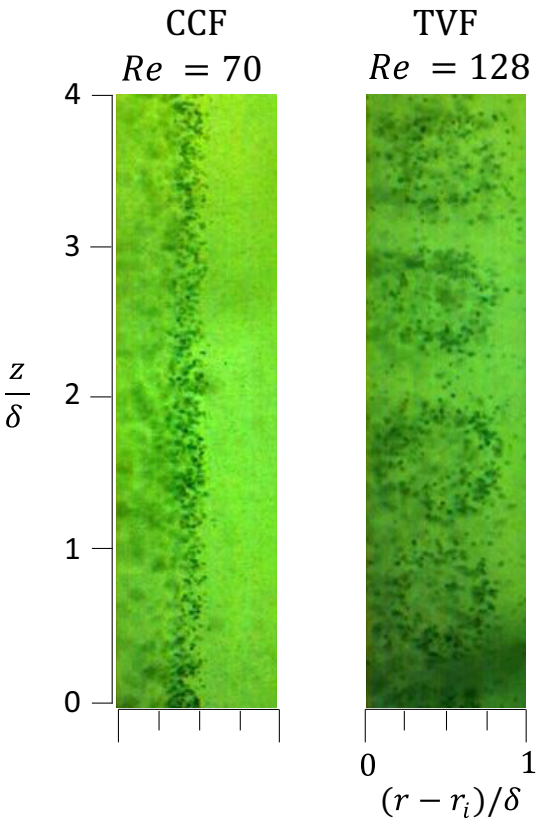

FIG. 3. Steady-state equilibrium positions of particles in the radial axial (r-z) plane in the circular Couette flow (left panel) and Taylor vortex flow (right panel) for a suspension of $\phi = 0.01$ and $d_p \approx 230$ μm. Dark and sharp spots are the particles in the plane of interest. Some out-of-plane particles can be seen as lighter blurred spots. For a suspension with $\phi = 0.01$, the CCF is stable for $0 < \mathrm{Re} < 120$ and TVF is stable for $120 < \mathrm{Re} < 152$ in the TC geometry considered here.

were taken from one side of the Taylor-Couette apparatus to record particle locations in the radial-axial (r-z) plane as detailed in prior work [28]. In CCF, particles migrate toward the middle of the annular region with a slight offset toward the inner cylinder. In the TVF regime, particles accumulate on a roughly circular region in the r-z plane within each vortex. The concentration fields following migration illustrated in Fig. 3 agree with the results presented in Ref. [28] for a more dilute suspension of $\phi = 0.001$. Based on the results observed in these experiments, it was determined that a time period of $t = 50$ min is sufficient for particle distributions to reach a state of full migration in the respective flow state for all Re considered in this work. Particles are expected to migrate faster at higher Re and because of the competition with fluctuations leading to diffusion, higher particle concentrations may also reach the final concentration field more rapidly.

3. Flow transition boundaries

The initial and final states for all the experiments presented in this paper are marked on the flow transition map for quasisteady increasing-Re [Fig. 4(a)] and decreasing-Re [Fig. 4(b)] ramps. The map, reproduced here with modifications from Majji *et al.* [14], shows Re corresponding to various flow structures and transitions for a suspension at $\phi = 0.10$ for slowly ramped conditions, i.e., $d\mathrm{Re}/d\tau \ll 1$, where the time is nondimensionalized as $\tau = t/t_d$ using a diffusion time scale

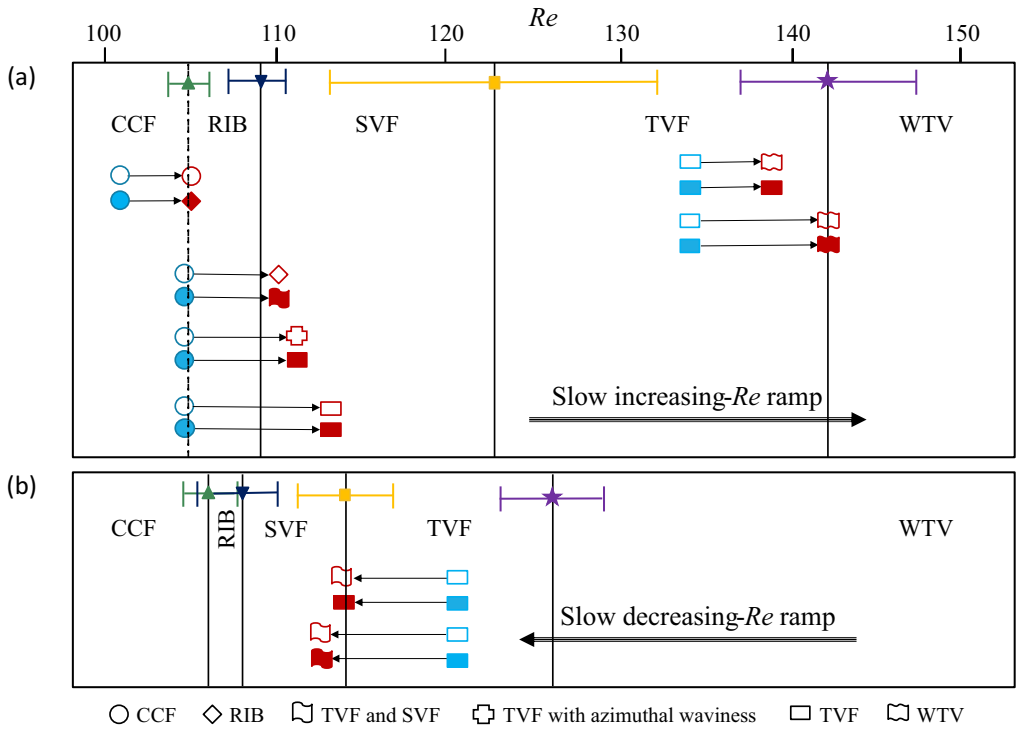

FIG. 4. Flow transition map for slowly ramped conditions showing Re corresponding to various flow structures and transitions for $\phi = 0.10$ suspension with particles of size $d_p \approx 230$ μm during (a) increasing-Re ramp with $d\mathrm{Re}/d\tau = 0.0031$, and (b) decreasing-Re ramp with $d\mathrm{Re}/d\tau = -0.0031$; here $\tau = t/t_d$. Vertical lines with the following symbols ▲, ▼, ■, ★ correspond to the average transition Re for CCF ↔ RIB, RIB ↔ SVF, SVF ↔ TVF, and TVF ↔ WTV transitions, respectively. Error bars show the standard deviation from the average value of transition Re. Adapted from Fig. 10 in Ref. [14]. The initial and final states for all experiments discussed in this work are marked on the flow transition map. Open symbols correspond to experiments with uniform suspension concentration at the initial state and filled symbols to experiments with inertially migrated particle concentration at the initial state. Different symbols are used for different flow structures observed in the experiments discussed in Sec. III.

$t_d = (\delta^2\rho)/\mu_s$. We chose the work of Majji *et al.* [14] to compare our work against because our experimental apparatus is the one used in that work. Open symbols correspond to experiments with uniform suspension concentration at the initial state and filled symbols to experiments with inertially migrated particle distribution at the initial state. Different symbols are used for different flow structures observed in the rapid Re step change experiments discussed in Sec. III. Note that at a given Re, the final flow structure in our experiments might differ from the one observed in slowly ramped conditions at the same Re due to the different experimental protocol utilized here. The rapid Re step change protocol introduces an inertial jump effect, which is not present in the slowly ramped conditions. The manner in which the desired Re is reached, i.e., the protocol for change of Re, plays an important role in the flow structure accessed and the critical condition observed [30]. In slowly increasing-Re ramp experiments performed previously [14], the CCF-RIB transition was not captured as their experiments started at Re that is above this transition. Quasisteady increasing-Re experiments starting at Re corresponding to CCF were performed to capture the CCF-RIB transition. The experiments were repeated four times and the average CCF-RIB transition Re with error bars

showing the standard deviation from the average value of transition Re is shown as a dashed line in Fig. 4(a).

It is clear from Fig. 4 that flow transitions exhibit significant hysteresis. For a suspension of $\phi = 0.10$, Majji *et al.* [14] showed that flow transitions during an increasing-Re ramp are qualitatively the same but quantitatively different from those observed during a decreasing-Re ramp. The WTV-TVF and TVF-SVF transitions were observed to occur at higher Re during a ramp-up protocol compared to ramp-down, indicating hysteresis in flow transitions. Note that in the slowly increasing- and decreasing-Re ramps (quasisteady) experiments in previous studies [14,15,17], the concentration profile at any Re corresponds closely to the steady distribution with full migration, except perhaps at conditions just above or below a transition. Experiments described in the current work for conditions of uniform concentration distribution thus provide information on system dynamics distinct from the past quasi-steady experiments. By comparison to results for suspensions subject to inertial migration, our observations thus provide insight into the influence of concentration variation on hysteresis.

An initial estimate of the transition boundary (Re_c) for flow transitions considered in this study is obtained from the slowly ramped conditions shown in Fig. 4. For the CCF-nonaxisymmetric flow transition, a natural choice for the initial value of Re_c is based on increasing-Re ramp experiments in which the observed transition Reynolds away from the CCF corresponds to inertially migrated concentration in CCF. For the TVF-WTV transition, the initial estimate of Re_c is set to the TVF-WTV transition Re obtained from increasing-Re ramp experiments. This Reynolds number corresponds to the transition Re to WTV for a suspension with inertially migrated concentration field in TVF, forming elevated-ϕ rings in each vortex. For the TVF-nonaxisymmetric flow transition, an initial estimate of Re is set to the critical condition for TVF-SVF obtained in slowly decreasing-Re ramp experiments. This condition corresponds to the lower limit Re of TVF for a fully migrated suspension in this flow state.

All Re_c estimates are then refined by performing multiple rapid small step changes in Re to define the transition interval for the experiments discussed in this work. In the Re_1 to Re_2 step change protocol used in this work, the Re change is about 5% of Re_1 and the experiment is repeated multiple times with slight changes to Re_1 and Re_2 to refine the estimate of the transition boundary and locate the Re interval over which flow transition takes place. Figure 5 shows the flow transition map with this new Re step change protocol, where gray shaded regions represent the region over which flow transition is observed. Note that the differences in the transition boundaries between Fig. 4 and Fig. 5 are primarily due to the difference in the protocols for change of Re. We recall that a change of Re in all cases is achieved by change in inner cylinder rotation rate, maintaining fixed outer cylinder.

The results of experiments with a suspension of PMMA particles of size $d_p \approx 230\ \mu$m and at a concentration of $\phi = 0.10$ will be discussed in detail in the following sections. Here, inertia is present both in bulk and at particle scale as the bulk flow Reynolds number is $\mathrm{Re} > 100$ and the particle scale Reynolds number is $\mathrm{Re}_p \geqslant 0.03$. Rather than the sequence seen in pure fluid with only inner cylinder rotating, of CCF to TVF to WTV with increasing Re [6], a more complex and hysteretic sequence is found for the suspension flow as discussed above. To explore this set of transitions, we first describe in Sec. III A the effect of inertial migration in CCF on the CCF-nonaxisymmetric flow (SVF and RIB) transition, which with further increase of Re gives way to TVF. Having established this behavior for entry into TVF as Re increases, we then consider in Sec. III B 1 the role of migration in the vortex structures on the upper limit transition away from TVF to WTV. With these results established, we finally consider the influence of inertial migration on the transition from TVF to the nonaxisymmetric flow states (SVF and RIB) at the lower limit of Re for TVF, in Sec. III B 2.

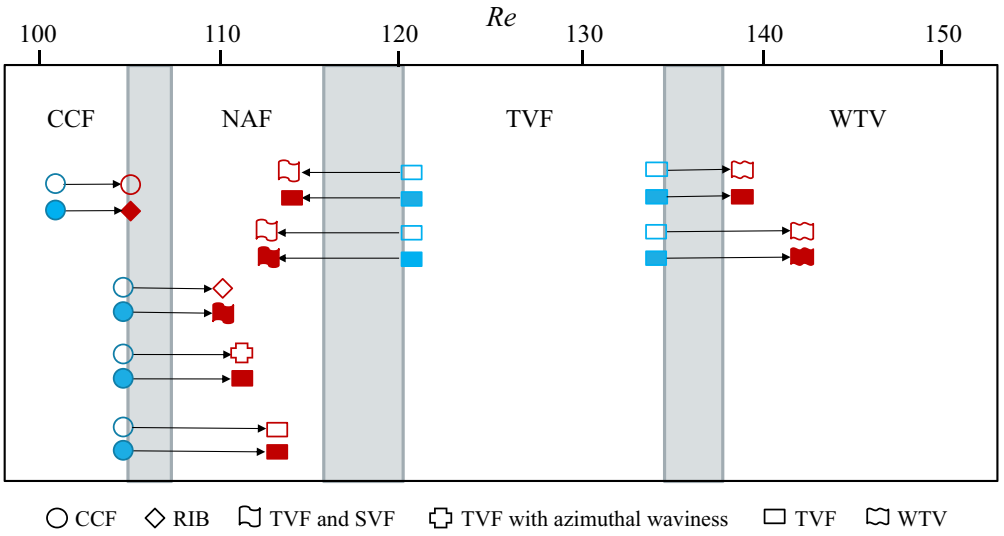

FIG. 5. Flow transition map for rapid Re step change experiments showing Re corresponding to various flow structures and transitions for $\phi = 0.10$ suspension with particles of size $d_p \approx 230\ \mu$m. The rate of Re step change ranges from $d\mathrm{Re}/d\tau = 3.4$ to $d\mathrm{Re}/d\tau = 6.7$ for Re step increase experiments, and from $d\mathrm{Re}/d\tau = -5.3$ to $d\mathrm{Re}/d\tau = -6.3$ for Re step decrease experiments; here $\tau = t/t_d$. Gray shaded regions show the range of Re over which flow transition away from the initial flow state is observed for the experiments considered in this work. The initial and final states for all experiments discussed in this work are marked on the flow transition map. Open symbols correspond to experiments with uniform suspension concentration at the initial state and filled symbols to experiments with inertially migrated particle concentration at the initial state. Different symbols are used for different flow structures observed in the experiments discussed in Sec. III.

III. RESULTS AND DISCUSSION

A. Transition from circular Couette flow

For $\phi = 0.10$, we first establish circular Couette flow (CCF) states at a desired inner cylinder Reynolds number of Re_1 for the two initial states: (I) negligible migration, i.e., with uniform particle distribution, and (II) full migration, with a steady particle distribution following inertial migration. The Reynolds number is then rapidly (essentially instantaneously as compared to prior results with slow ramp rate [28]) increased to a specific value, $\mathrm{Re}_2 = \mathrm{Re}_1 + \Delta\mathrm{Re}$, and held there for 50 min. We observe the evolution of the flow structures between the two cases I and II.

Starting with a quiescent well-mixed suspension, the inner cylinder rotation rate was increased rapidly from rest to the desired Re_1 in the CCF regime. In case I, the flow was held for only 1 min to avoid inertial migration and have a nearly uniform concentration. Note that the diffusion time scale here is $t_d \approx 1.8\ s$, significantly shorter than the 1 min wait duration at Re_1. In case II, the flow was held at Re_1 for 50 min to allow for full migration. At the dilute concentration of $\phi = 0.01$ in CCF, interaction of flow disturbances due to particles with cylinder walls and the shear gradient of the underlying flow pushes the particles to form a narrow distribution near the center of the annular region as shown in Fig. 3. At $\phi = 0.10$, migration results in locally higher concentrations near the center of the annular region leading to the interaction of flow disturbances created by particles, which generate a diffusion and thus resist further particle migration. This yields a broader concentration distribution across the annular width. The opaqueness at the higher $\phi = 0.10$ combined with the curvature of the Taylor-Couette flow do not allow us to obtain quality visualization and accurate measurement of the radial particle distribution. Ramesh *et al.* [15] observed the formation of shear-band-type azimuthal velocity v_θ profiles across the Couette gap

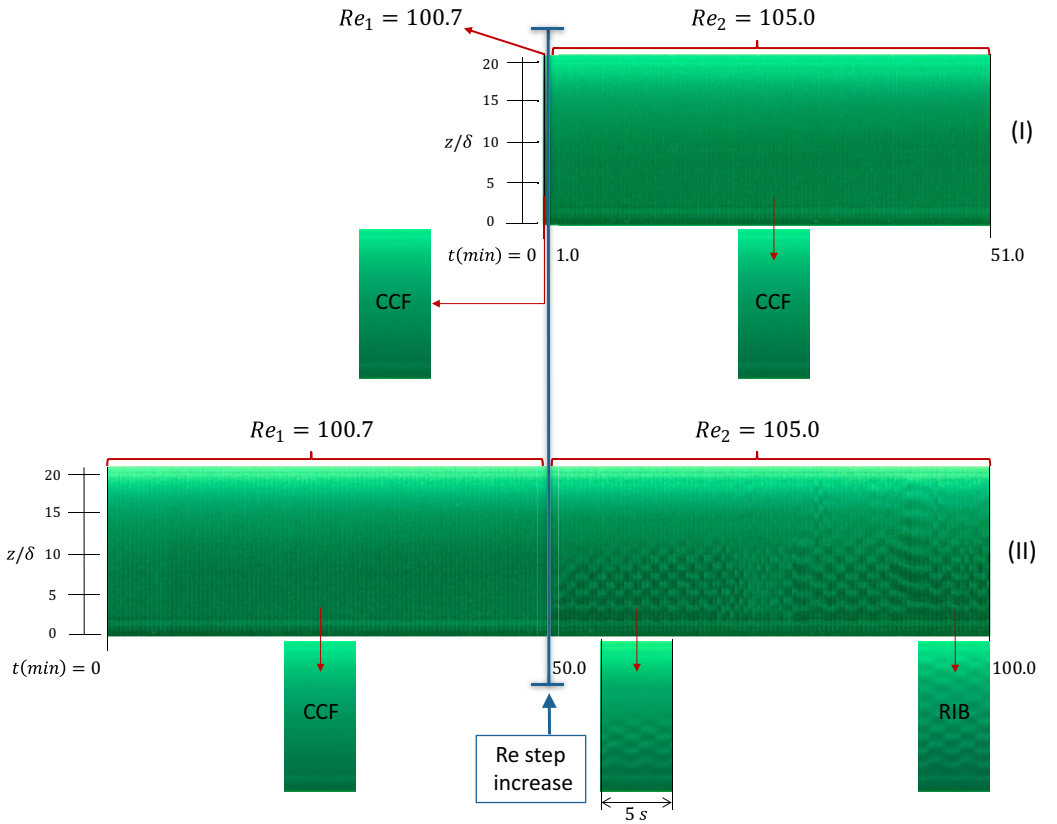

FIG. 6. Time evolution of flow structures for a $\phi = 0.10$ suspension when Re is rapidly increased from a circular Couette flow from Re = 100.7 to Re = 105. Two cases with different particle concentration profiles in CCF just before imposing the Re step change are presented: (I) uniformly distributed (II) steady inertially migrated distribution. Vertical blue line indicates the time of Re step increase. Shown are the flow evolution for 50 min after the Re increase for cases (I) and (II) and flow evolution for 1 min in case (I) and 50 min in case (II) before the Re increase.

in the CCF regime for suspensions of particle volume fraction $0.05 \leqslant \phi \leqslant 0.15$. They postulated that a shear-banded velocity profile is likely due to the accumulation of particles around the center of the Couette gap. In the current work, after 50 min at Re_1, the rotation rate of the inner cylinder was rapidly increased to Re_2 and kept constant for 50 min. This procedure was repeated for different combinations of Re_1 and Re_2 in the range $100.7 \leqslant \mathrm{Re} \leqslant 113.1$.

Images at low resolution of the flow structures were taken from the direction normal to the cylinder axis using the low speed camera at an interval of 40 s between frames for the entire duration of the experiment. At regular intervals, images were taken at 60 frames s^{-1} at high resolution for 5 s using the high-speed camera to capture the fully time-resolved flow structure. Space-time diagrams, which show the time evolution of the flow structures, were constructed from sequences of images by plotting the time evolution of an area 16 pixel width by full axial height near the image center.

Figure 6(I), for example, shows the space-time diagram (vertical axis is height and horizontal axis is time) constructed from the low-resolution images. This is for an experiment in which CCF of a $\phi = 0.10$ suspension with uniform concentration distribution is held at $\mathrm{Re}_1 = 100.7$ for 1 min followed by rapid increase to $\mathrm{Re}_2 = 105$, at which it is held for 50 min. The CCF flow structure at the end of 1 min at $\mathrm{Re}_1 = 100.7$ is shown in the high-resolution space-time diagram below the

low-resolution diagram. The flow is CCF in the full length of the annulus with the exception of top and bottom Ekman layers. The flow at $\mathrm{Re}_2 = 105$ stays as CCF for the full duration of 50 min.

Figure 6(II) shows the space-time diagram for conditions similar to (I), but with $\mathrm{Re}_1 = 100.7$ held for 50 min rather than 1 min, to result in fully migrated particle distribution before imposing the rapid increase in Re. The high-resolution space-time diagrams at various times are shown below the low-resolution diagram. The flow remains in CCF for the entire duration of 50 min at $\mathrm{Re}_1 = 100.7$ and develops into ribbons flow structure (RIB) in the lower section of the annulus immediately following the increase in Re. The flow structure then evolves into RIB in the full axial length at 30 min after the rate change. Hence, when Re is abruptly increased from $\mathrm{Re}_1 = 100.7$ to $\mathrm{Re}_2 = 105$, the uniform particle distribution in CCF led to no instability whereas the fully migrated particle distribution in CCF led to the onset of instability, with transition into a steady RIB flow structure. Note that in RIB, the particles are well mixed as the time modulation of the flow is much faster than the inertial migration time scale.

Space-time diagrams for the same flow protocols as just described, now with $(\mathrm{Re}_1, \mathrm{Re}_2) = (104.6, 110.1)$, (104.6, 111.0), and (104.6, 113.1), are shown in Figs. 7–9, respectively. The flow structure at the end of $\mathrm{Re}_1 = 104.6$ in Fig. 7 shows that the flow is CCF in the full annular length for both the suspensions with (I) uniform and (II) fully migrated concentration profiles. Following the increase of Re to $\mathrm{Re}_2 = 110.1$, the suspension with the uniform concentration profile (case I) remained in CCF for a duration of approximately 25 min, after which time the RIB structure developed in the lower section of the annulus. This evolved into a full length RIB flow by the end of 50 min. In contrast, for the case of the suspension with full migration (II), the flow went unstable immediately after the increase in Re, to form a flow structure with Taylor vortices in the lower half of the annulus and spiral vortices in the upper half. The vortices near the middle resulting from merging of the two structures showed azimuthal waviness. This flow structure remained until the end of 50 min at $\mathrm{Re}_2 = 110.1$.

When the Re is rapidly increased from $\mathrm{Re}_1 = 104.6$ to $\mathrm{Re}_2 = 111.0$, the CCF flow goes unstable immediately for both cases, as shown in Fig. 8, but the two cases go unstable to different flow structures. During the 50 min at $\mathrm{Re}_2 = 111.0$, the suspension with uniform concentration begins in spiral vortices in the full axial length, evolving to a combination of Taylor vortices and spiral vortices, and finally to Taylor vortices with azimuthal waviness in the entire annulus. In the case of full migration to nonuniform concentration, the flow structures evolve from spiral vortex flow immediately after increase of Re to Taylor vortex flow by the end of 50 min at $\mathrm{Re}_2 = 111.0$.

From Figs. 6–8, we see that the flow transition away from the base CCF at $\phi = 0.10$ takes place at a lower Re when migration has occurred than for uniform concentration. Hence, the particle distribution resulting from inertial migration destabilizes CCF of suspensions. For inertial migration in CCF, the nonaxisymmetric flow states (ribbons and spirals) between CCF and Taylor vortex flow (TVF) reported by Majji *et al.* [14] with a quasisteady decreasing Re protocol were also observed here.

Finally, Fig. 9 shows the flow transitions from CCF when Re is increased from $\mathrm{Re}_1 = 104.6$ to $\mathrm{Re}_2 = 113.1$. The flow destabilizes immediately after Re increase in both uniform and migrated cases and follows a similar sequence of flow structures: spirals to a combination of spirals and Taylor vortices, and finally to Taylor vortex flow. This increase in Re is apparently sufficiently large to eliminate the effect of concentration variation. Repeated experiments with $(\mathrm{Re}_1, \mathrm{Re}_2)$ in the vicinity of the CCF-NAF transition boundary (Fig. 5) confirmed the destabilizing effect of nonuniform concentration due to particle migration in the CCF when compared to the uniform suspension case.

B. Transition from Taylor vortex flow

1. Upper limit of Re for Taylor vortex flow

For a Newtonian fluid in the apparatus used in this work, Taylor vortex flow (TVF) is stable for $120 < \mathrm{Re} < 152$ and transitions into CCF for $\mathrm{Re} < 120$ and wavy Taylor vortex flow (WTV) for

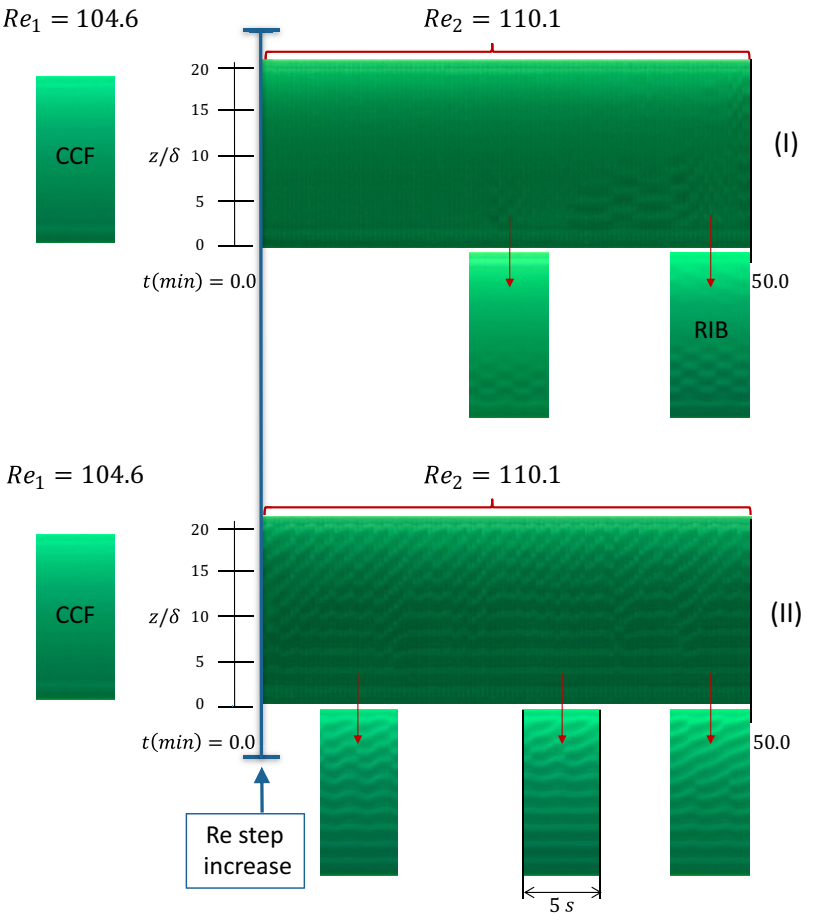

FIG. 7. Time evolution of flow structures for a $\phi = 0.10$ suspension when Re is rapidly increased from a circular Couette flow from Re = 104.6 to Re = 110.1. Two cases with different particle concentration profiles in CCF just before imposing the Re step change are presented: (I) uniformly distributed, and (II) steady inertially migrated distribution. Vertical blue line indicates the time of Re step increase. The flow states before the Re step increase for cases (I) and (II) are shown to the left of the blue line. The flow evolution for 50 min after the Re increase for cases (I) and (II) are shown to the right of the blue line.

Re > 152. These values of Re change for a suspension. With $\phi = 0.10$ and $d_p \approx 230$ μm using a quasisteady increasing-Re protocol, Majji *et al.* [14] showed that the range of Re values for which TVF is stable is reduced significantly compared to the case of Newtonian fluid, with the range depending strongly on the flow protocol, as indicated by Fig 4; the flow transitioned into WTV for Re above this range, and to spiral vortex flow (SVF) for Re below this range (rather than directly to CCF as seen in the Newtonian fluid). Note that, in their experiments [14], the concentration profile at a given Re corresponds closely to the fully migrated distribution at that condition owing to the slow change in flow rate. The objective here is to gain further insight to hysteresis in suspension TC flow, by determining the effect of the particle migration on TVF-WTV and TVF-SVF flow transitions, relative to a uniform suspension. For this purpose, we follow a protocol different from Majji *et al.*.

Starting with a well-mixed suspension, the rotation rate of the inner cylinder was increased rapidly from rest to Re_1 to establish the Taylor vortex flow (TVF). In case I, the TVF was established

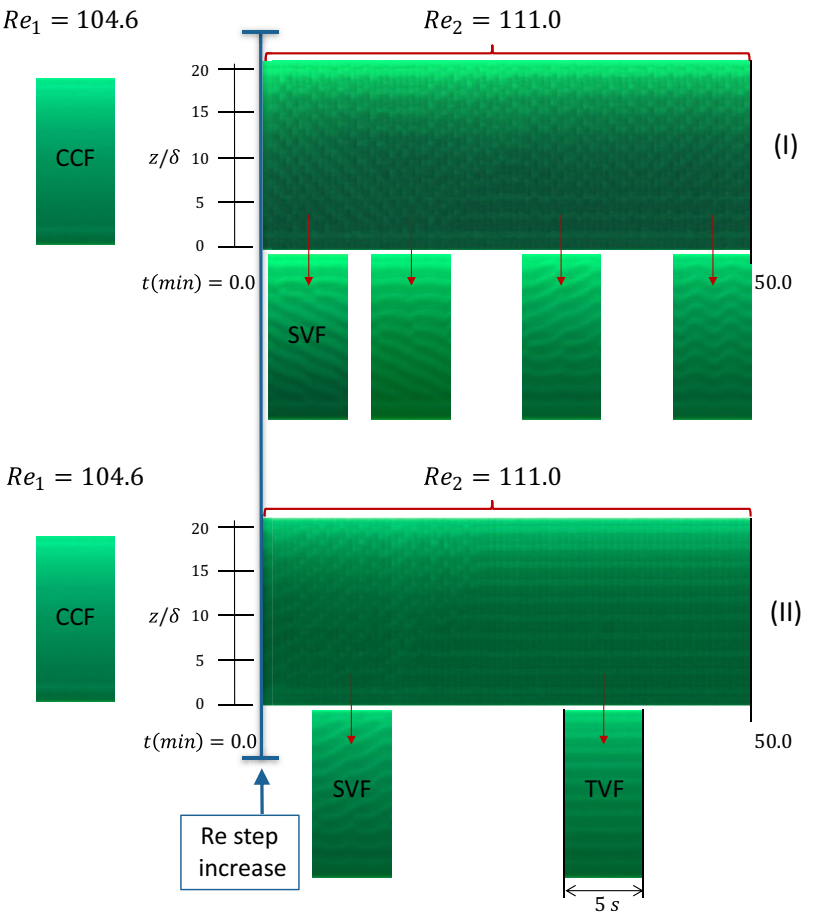

FIG. 8. Time evolution of flow structures for a $\phi = 0.10$ suspension when Re is rapidly increased from a circular Couette flow from Re = 104.6 to Re = 111.0. Two cases with different particle concentration profiles in CCF just before imposing the Re step change are presented: (I) uniformly distributed, (II) steady inertially migrated distribution. Vertical blue line indicates the time of Re step increase. The flow states before the Re step increase for cases (I) and (II) are shown to the left of the blue line. The flow evolution for 50 min after the Re increase for cases (I) and (II) are shown to the right of the blue line.

in the full annular length and held at Re_1 only for 1 min to retain a nearly uniform particle distribution. The inner cylinder Re was then changed as rapidly as the motor allowed to Re_2 and held at this condition for 50 min to observe the flow evolution. In case II, the rotation rate was held in TVF at Re_1 for 50 min to allow particles to migrate to a steady concentration profile in each Taylor vortex. In TVF of dilute suspensions, flow disturbances caused by individual particles interact with the confining walls and the underlying flow gradients of the vortex flow. As a result particles are simultaneously pushed away from the walls and vortex centers. This, in combination with the convective transport of the toroidal Taylor vortex, leads to particle accumulation on a circular limit cycle in each vortex, when seen in the radial-axial (r-z) plane as shown in Fig. 3 for $\phi = 0.01$. The diameter of this circular equilibrium region was previously observed to grow with increase in Re in the TVF regime [28]. For $\phi = 0.10$ as considered in this work, particle-particle hydrodynamic interactions in the relatively highly concentrated regions created by inertial migration leads to wider

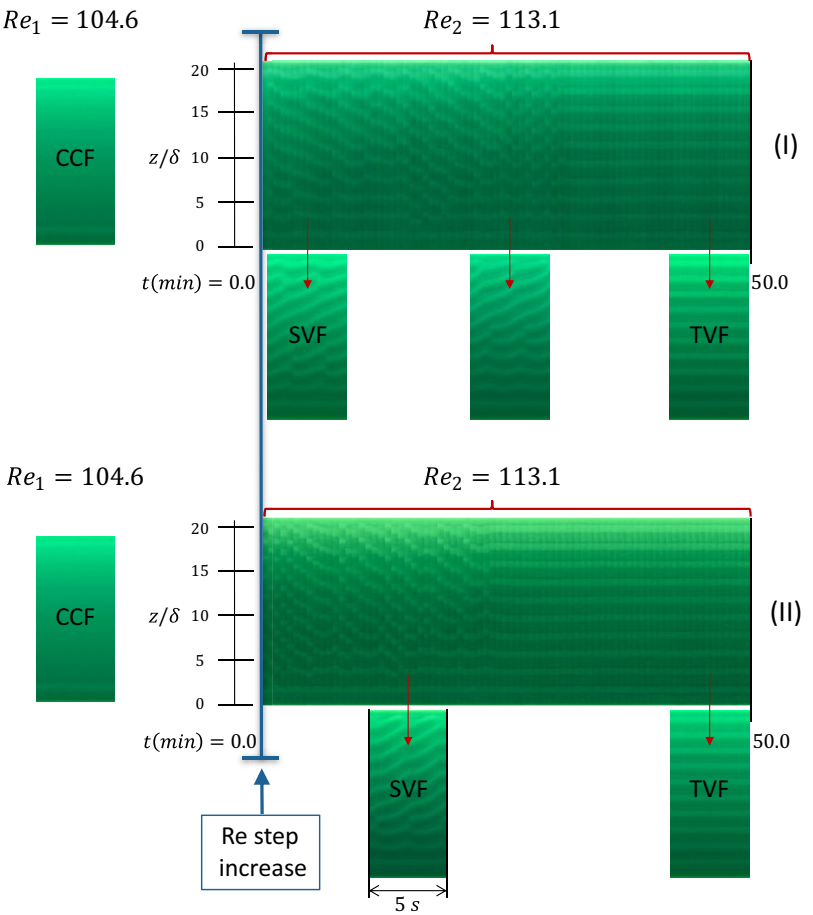

FIG. 9. Time evolution of flow structures for a $\phi = 0.10$ suspension when Re is rapidly increased from a circular Couette flow from Re = 104.6 to Re = 113.1. Two cases with different particle concentration profiles in CCF just before imposing the Re step change are presented: (I) uniformly distributed, (II) steady inertially migrated distribution. Vertical blue line indicates the time of Re step increase. The flow states before the Re step increase for cases (I) and (II) are shown to the left of the blue line. The flow evolution for 50 min after the Re increase for cases (I) and (II) are shown to the right of the blue line.

equilibrium concentration distributions around the limit cycles. After 50 min at Re_1, the rotation rate of the inner cylinder was rapidly changed to Re_2 and held for 50 min to observe the flow evolution.

Figures 10(a) and 10(b) show significant effect of the particle distribution in TVF on the TVF-WTV flow transition. Space-time diagrams in Fig. 10(a) [case (I)] show time evolution of flow structure when the suspension flow is held at $\mathrm{Re}_1 = 134.1$ for 1 min followed by a rapid increase in Re to $\mathrm{Re}_2 = 138.7$ where it was held for 50 min. The flow just before the Re increase was the TVF with particles uniformly distributed across the vortices. Following the Re increase, the flow became unstable after approximately 3 min and transitioned to WTV, remaining in this flow state until the end of 50 min at Re_2; the WTV consists of vortices in the full annulus length with traveling waves propagating along the azimuthal direction. When the TVF at $\mathrm{Re}_1 = 134.1$ was held for 50 min to allow for inertial migration, the resultant time evolution of flow structures is shown in the space-time diagrams in Fig. 10(a) [case (II)]. This shows that following the Re increase, the TVF state remains stable until the end of 50 min at Re_2. Particle migration in the

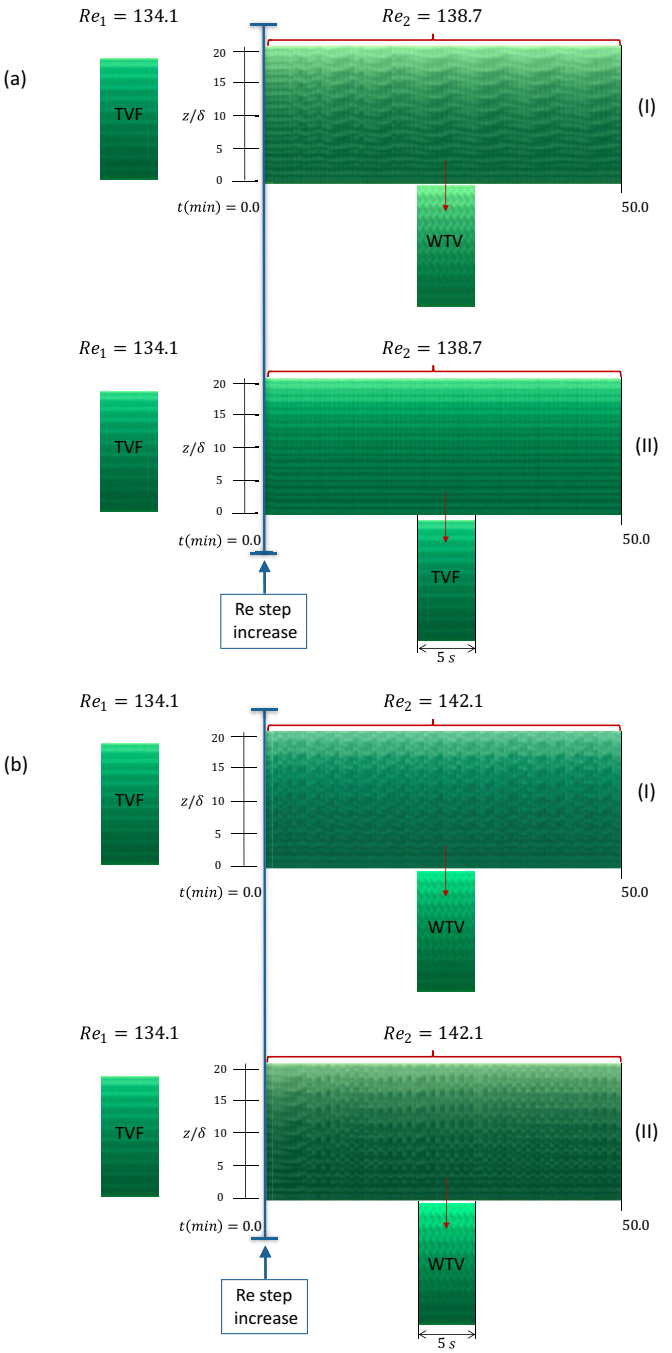

FIG. 10. Time evolution of flow structures for a $\phi = 0.10$ suspension when Re is rapidly increased from a Taylor vortex flow (TVF): (a) from Re $= 134.1$ to Re $= 138.7$, (b) from Re $= 134.1$ to Re $= 142.1$. Two cases with different particle concentration profiles in TVF just before imposing the Re step change are presented: (I) uniformly distributed, (II) steady inertially migrated distribution. Vertical blue line indicates the time of Re step increase. The flow states before the Re step increase for cases (I) and (II) are shown to the left of the blue line. The flow evolution for 50 min after the Re increase for cases (I) and (II) are shown to the right of the blue line.

TVF regime thus has a stabilizing effect to increasing Re as opposed to the destabilizing effect of inertial migration in the CCF regime. Due to inertial migration in the TVF regime, particles are focused to the zone near the circular limit cycle found for dilute conditions, and the inertia at $\mathrm{Re}_2 = 138.7$ is not strong enough to destabilize the TVF with this arrangement of particles. For the same experimental protocol, but with Reynolds number increased to a higher value, from $\mathrm{Re}_1 = 134.1$ to $\mathrm{Re}_2 = 142.1$ [Fig. 10(b)], both the TVF with uniform particle distribution (I) and the TVF with full inertial migration (II) transition into WTV. The WTV then remained for the 50 min duration at Re_2. The results of Figs. 10(a) and 10(b) show that the TVF with migrated concentration profile transitions into WTV at higher Re compared to the TVF with uniform particle distribution. Majji *et al.* [14] and Ramesh *et at.* [15] compared flow transitions and flow structures of a suspension during a quasi-steady decreasing-Re ramp with those observed from a quasisteady increasing-Re ramp. Both found flow transition from TVF into WTV during the increasing-Re ramp occurred at higher Re compared to the transition during the decreasing-Re ramp ($\mathrm{Re}_c^{\mathrm{up}} > \mathrm{Re}_c^{\mathrm{down}}$), thus showing significant hysteresis. In a quasisteady increasing-Re ramp, particles spend enough time in the TVF to undergo inertial migration before transitioning into WTV. On the other hand, the system reaches the WTV-TVF transition with relatively uniform particle distribution during a decreasing-Re ramp. These considerations together with our experiments with uniform and nonuniform concentration show that migration in the TVF regime has a significant role in the hysteresis in WTV-TVF transitions observed with quasisteady Re ramping protocols.

2. Lower limit of Re for Taylor vortex flow

The effects of the particle distribution in TVF on the TVF-SVF flow transition are shown in Fig. 11. When Re was quickly decreased to $\mathrm{Re}_2 = 113.7$ after holding the TVF at $\mathrm{Re}_1 = 120.5$ for 1 min, the flow immediately underwent a transition into the RIB state, which then evolved into a state with spiral vortices merging into Taylor vortices with azimuthal waviness. This latter mixed state remained to the end of the experiment, as shown in the uniform concentration profile case (I) in Fig. 11(a).

When the TVF at $\mathrm{Re}_1 = 120.5$ was held for 50 min instead of 1 min to allow for inertial migration, followed by rapid reduction of Re, the space-time diagrams in Fig. 11(a) [case (II)] show that the top section of the TVF flow destabilized to form spiral vortices for a short time immediately after the reduction of Re, but the flow recovered to, and remained in, TVF for the remainder of the experiment. Apparently, the nonuniform concentration distribution due to inertial migration has a stabilizing effect on the TVF and results in a lower TVF-SVF transition Re compared to the well-mixed suspension case. Figure 11(b) shows the results for a similar experiment but with rapid reduction in Re from $\mathrm{Re}_1 = 120.5$ to $\mathrm{Re}_2 = 112.5$, slightly lower than the prior case. Both the TVF with uniform particle distribution (I) and TVF with migrated concentration profile (II) immediately underwent transitions into RIB, which then evolved into a combination of spiral and Taylor vortices with azimuthal waviness. This mixed state remained until the end of the experiment. The results of Figs. 11(a) and 11(b) show that the TVF-SVF transition Re is lower for nonuniform concentration due to inertial migration. Majji *et al.* [14] previously observed that for quasisteady Re ramp experiments, the transition from TVF to SVF took place at a lower Re in quasisteady Re ramp-down experiments compared to the value observed in Re ramp-up experiments. Again, the results of our experiments suggest this hysteresis in the TVF-SVF transition from the Majji *et al.* study, at least for $\phi \leqslant 0.10$, is a result of particle migration to the vortex limit cycle zones in the TVF regime.

Results presented in this section show that the flow-induced structure due to particle migration in the TVF regime results in a history-dependent flow system and increases the range of Re over which the TVF is stable. A higher onset Re was observed for the transition from TVF to WTV and a lower onset Re was observed for the transition from the TVF to nonaxisymmetric flow (NAF) structures when the particle distribution was nonuniform due to inertial migration in the TVF regime. The transition away from TVF thus exhibits hysteresis at both of these regime boundaries. Repeated

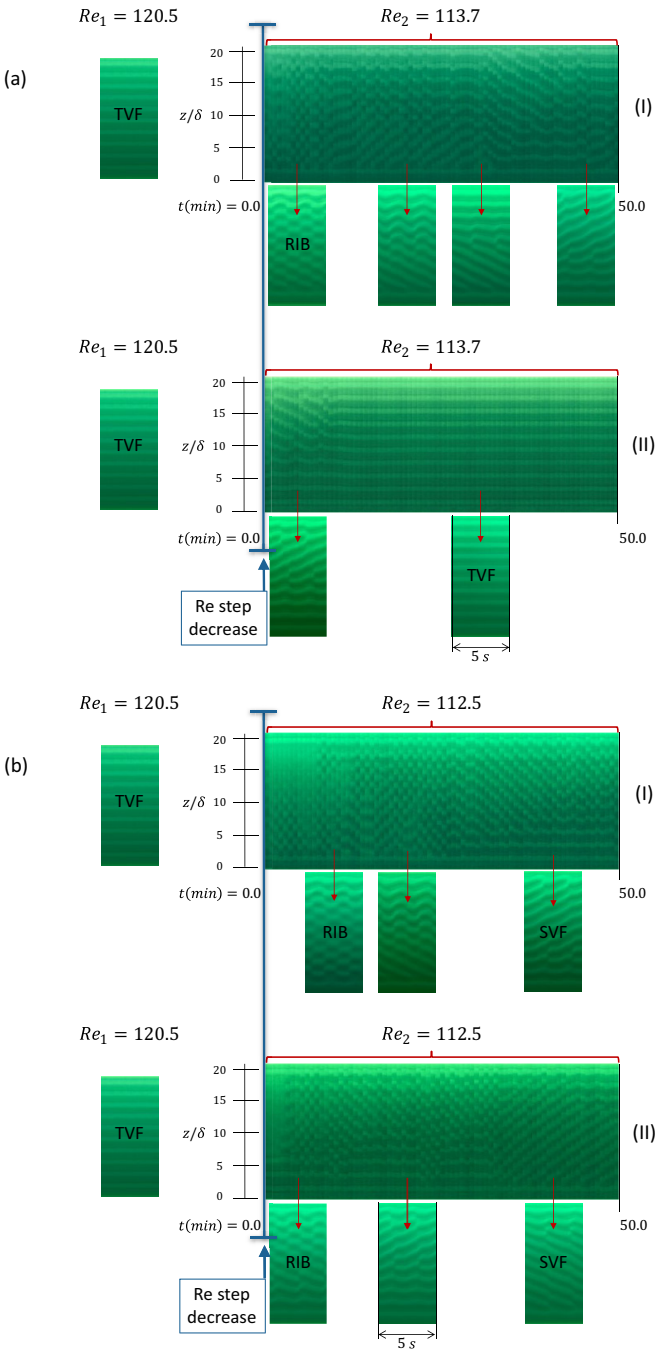

FIG. 11. Time evolution of flow structures for a $\phi = 0.10$ suspension when Re is rapidly decreased from a Taylor vortex flow (TVF): (a) from Re $= 120.5$ to Re $= 113.7$, (b) from Re $= 120.5$ to Re $= 112.5$. Two cases with different particle concentration profiles in TVF just before imposing the Re step decrease are presented: (I) uniformly distributed, (II) steady inertially migrated distribution. Vertical blue line indicates the time of Re step decrease. The flow states before the Re step decrease for cases (I) and (II) are shown to the left of the blue line. The flow evolution for 50 min after the Re decrease for cases (I) and (II) are shown to the right of the blue line.

experiments for (Re_1, Re_2) in the vicinity of TVF-WTV and TVF-NAF transition boundaries (Fig. 5) confirmed the stabilizing effect of fully migrated concentration in TVF compared to uniform suspension.

IV. CONCLUSION

We have experimentally investigated the effect of inertial migration on flow transitions in suspension Taylor-Couette flow. This was considered for neutrally buoyant particles of size $d_p \approx 230\ \mu$m in the CCF and TVF flow states of a $\phi = 0.10$ suspension with a stationary outer cylinder and rotating inner cylinder. The hysteresis effects associated with particles were studied by considering the influence of nonuniform particle distribution due to particle migration in the initial flow state on various flow transitions (CCF-nonaxisymmetric, TVF-WTV, and TVF-SVF) and final flow states, relative to the case with uniform particle distribution. For each case studied here, two sets of experiments were performed. In the first set, a desired flow structure (CCF or TVF) near the transition boundary with uniformly distributed particles across the annulus was subjected to a rapid change in inner cylinder rotation rate, or Re. In the second set, the concentration distribution in the flow structure just before the Re change corresponded to the fully migrated particle distribution.

The key finding of this work is that, compared to the uniform particle distribution, the inertially migrated concentration profile destabilized the CCF state near the CCF-nonaxisymmetric flow transition boundary whereas it stabilized the TVF flow near TVF-WTV and TVF-SVF transition boundaries. The observed flow structures following the flow transition are in line with the earlier works by Majji *et al.* [14] and Ramesh *et at.* [15]. Quasisteady increasing- and decreasing-Re protocols were imposed in their studies and hysteretic behavior was reported for values of various transition Reynolds numbers between the two protocols. Note that the concentration profiles in the flow states in their work just before the flow transitions corresponded to the fully migrated particle distribution. Comparison of results of the present work between the cases with uniform particle distribution and fully migrated distribution show that concentration variation has a significant effect in causing the hysteretic behavior. The current work in combination with the stabilizing effect of nonuniform viscosity profile in CCF as indicated by the linear stability analysis of Majji *et al.* [14] suggests that a focus should be made in future work on the mechanism by which nonuniformly distributed particles leads to the various destabilizing and stabilizing effects observed in suspension Taylor-Couette flows. Quantitative measurement of the concentration profiles in the annular region in CCF and TVF prior to the transition is a natural next step in that direction.

[1] G. I. Taylor, Viii. Stability of a viscous liquid contained between two rotating cylinders, Philos. Trans. R. Soc. London A **223**, 289 (1923).

[2] S. Chandrasekhar, The stability of viscous flow between rotating cylinders, Proc. R. Soc. London A **246**, 301 (1958).

[3] D. Coles, Transition in circular Couette flow, J. Fluid Mech. **21**, 385 (1965).

[4] T. Mullin and T. B. Benjamin, Transition to oscillatory motion in the Taylor experiment, Nature (London) **288**, 567 (1980).

[5] A. Lorenzen, G. Pfister, and T. Mullin, End effects on the transition to time-dependent motion in the Taylor experiment, Phys. Fluids **26**, 10 (1983).

[6] C. D. Andereck, S. Liu, and H. L. Swinney, Flow regimes in a circular Couette system with independently rotating cylinders, J. Fluid Mech. **164**, 155 (1986).

[7] S. T. Wereley and R. M. Lueptow, Spatio-temporal character of non-wavy and wavy Taylor–Couette flow, J. Fluid Mech. **364**, 59 (1998).

[8] O. Czarny, E. Serre, P. Bontoux, and R. M. Lueptow, Spiral and wavy vortex flows in short counter-rotating Taylor–Couette cells, Theor. Comput. Fluid Dyn. **16**, 5 (2002).

[9] C. Hoffmann, M. Lücke, and A. Pinter, Spiral vortices and Taylor vortices in the annulus between rotating cylinders and the effect of an axial flow, Phys. Rev. E **69**, 056309 (2004).
[10] R. G. Larson, E. S. Shaqfeh, and S. J. Muller, A purely elastic instability in Taylor–Couette flow, J. Fluid Mech. **218**, 573 (1990).
[11] S. Muller, E. Shaqfeh, and R. Larson, Experimental studies of the onset of oscillatory instability in viscoelastic Taylor-Couette flow, J. Non-Newtonian Fluid Mech. **46**, 315 (1993).
[12] N. Ashrafi and R. E. Khayat, Shear-thinning-induced chaos in Taylor-Couette flow, Phys. Rev. E **61**, 1455 (2000).
[13] N. Cagney and S. Balabani, Taylor-Couette flow of shear-thinning fluids, Phys. Fluids **31**, 053102 (2019).
[14] M. V. Majji, S. Banerjee, and J. F. Morris, Inertial flow transitions of a suspension in Taylor-Couette geometry, J. Fluid Mech. **835**, 936 (2018).
[15] P. Ramesh, S. Bharadwaj, and M. Alam, Suspension Taylor–Couette flow: Co-existence of stationary and traveling waves, and the characteristics of Taylor vortices and spirals, J. Fluid Mech. **870**, 901 (2019).
[16] M. E. Ali, D. Mitra, J. A. Schwille, and R. M. Lueptow, Hydrodynamic stability of a suspension in cylindrical Couette flow, Phys. Fluids **14**, 1236 (2002).
[17] P. Ramesh and M. Alam, Interpenetrating spiral vortices and other coexisting states in suspension Taylor-Couette flow, Phys. Rev. Fluids **5**, 042301 (2020).
[18] G. Segre and A. Silberberg, Behaviour of macroscopic rigid spheres in Poiseuille flow part 1. determination of local concentration by statistical analysis of particle passages through crossed light beams, J. Fluid Mech. **14**, 115 (1962).
[19] G. Segre and A. Silberberg, Behaviour of macroscopic rigid spheres in Poiseuille flow part 2. experimental results and interpretation, J. Fluid Mech. **14**, 136 (1962).
[20] B. Ho and L. Leal, Inertial migration of rigid spheres in two-dimensional unidirectional flows, J. Fluid Mech. **65**, 365 (1974).
[21] J. A. Schonberg and E. Hinch, Inertial migration of a sphere in Poiseuille flow, J. Fluid Mech. **203**, 517 (1989).
[22] E. S. Asmolov, The inertial lift on a spherical particle in a plane Poiseuille flow at large channel Reynolds number, J. Fluid Mech. **381**, 63 (1999).
[23] J.-P. Matas, J. F. Morris, and E. Guazzelli, Lateral force on a rigid sphere in large-inertia laminar pipe flow, J. Fluid Mech. **621**, 59 (2009).
[24] J. F. Morris and F. Boulay, Curvilinear flows of noncolloidal suspensions: The role of normal stresses, J. Rheol. **43**, 1213 (1999).
[25] D. R. Mikulencak and J. F. Morris, Stationary shear flow around fixed and free bodies at finite Reynolds number, J. Fluid Mech. **520**, 215 (2004).
[26] J. Halow and G. Wills, Experimental observations of sphere migration in Couette systems, Ind. Eng. Chem. Fundam. **9**, 603 (1970).
[27] S. T. Wereley and R. M. Lueptow, Inertial particle motion in a Taylor Couette rotating filter, Phys. Fluids **11**, 325 (1999).
[28] M. V. Majji and J. F. Morris, Inertial migration of particles in Taylor-Couette flows, Phys. Fluids **30**, 033303 (2018).
[29] M. Han, C. Kim, M. Kim, and S. Lee, Particle migration in tube flow of suspensions, J. Rheol. **43**, 1157 (1999).
[30] C. S. Dutcher and S. J. Muller, Spatio-temporal mode dynamics and higher order transitions in high aspect ratio Newtonian Taylor-Couette flows, J. Fluid Mech. **641**, 85 (2009).